Study of the structure of $e^+e^- \to b\bar{b}g$ events and first limits on the anomalous chromomagnetic coupling of the b quark

Kenji Abe,[21] Koya Abe,[33] T. Abe,[29] I. Adam,[29] H. Akimoto,[29] T. Akagi,[29] N. J. Allen,[5] W. W. Ash,[29] D. Aston,[29] K. G. Baird,[17] C. Baltay,[40] H. R. Band,[39] M. B. Barakat,[16] O. Bardon,[19] T. L. Barklow,[29] G. L. Bashindzhagyan,[20] J. M. Bauer,[18] G. Bellodi,[23] R. Ben-David,[40] A. C. Benvenuti,[3] G. M. Bilei,[25] D. Bisello,[24] G. Blaylock,[17] J. R. Bogart,[29] G. R. Bower,[29] J. E. Brau,[22] M. Breidenbach,[29] W. M. Bugg,[32] D. Burke,[29] T. H. Burnett,[38] P. N. Burrows,[23] A. Calcattera,[12] D. Calloway,[29] B. Camanzi,[11] M. Carpinelli,[26] R. Cassell,[29] R. Castaldi,[26] A. Castro,[24] M. Cavalli-Sforza,[35] A. Chou,[29] E. Church,[38] H. O. Cohn,[32] J. A. Coller,[6] M. R. Convery,[29] V. Cook,[38] R. Cotton,[5] R. F. Cowan,[19] D. G. Coyne,[35] G. Crawford,[29] C. J. S. Damerell,[27] M. N. Danielson,[8] M. Daoudi,[29] N. de Groot,[4] R. Dell'Orso,[25] P. J. Dervan,[5] R. de Sangro,[12] M. Dima,[10] A. D'Oliveira,[7] D. N. Dong,[19] M. Doser,[29] R. Dubois,[29] B. I. Eisenstein,[13] V. Eschenburg,[18] E. Etzion,[39] S. Fahey,[8] D. Falciai,[12] C. Fan,[8] J. P. Fernandez,[35] M. J. Fero,[19] K. Flood,[17] R. Frey,[22] J. Gifford,[36] T. Gillman,[27] G. Gladding,[13] S. Gonzalez,[19] E. R. Goodman,[8] E. L. Hart,[32] J. L. Harton,[10] A. Hasan,[5] K. Hasuko,[33] S. J. Hedges,[6] S. S. Hertzbach,[17] M. D. Hildreth[29] J. Huber,[22] M. E. Huffer,[29] E. W. Hughes,[29] X. Huynh,[29] H. Hwang,[22] M. Iwasaki,[22] D. J. Jackson,[27] P. Jacques,[28] J. A. Jaros,[29] Z. Y. Jiang,[29] A. S. Johnson,[29] J. R. Johnson,[39] R. A. Johnson,[7] T. Junk,[29] R. Kajikawa,[21] M. Kalelkar,[28] Y. Kamyshkov,[32] H. J. Kang,[28] I. Karliner,[13] H. Kawahara,[29] Y. D. Kim,[30] M. E. King,[29] R. King,[29] R. R. Kofler,[17] N. M. Krishna,[8] R. S. Kroeger,[18] M. Langston,[22] A. Lath,[19] D. W. G. Leith,[29] V. Lia,[19] C. Lin,[17] M. X. Liu,[40] X. Liu,[35] M. Loreti,[24] A. Lu,[34] H. L. Lynch,[29] J. Ma,[38] G. Mancinelli,[28] S. Manly,[40] G. Mantovani,[25] T. W. Markiewicz,[29] T. Maruyama,[29] H. Masuda,[29] E. Mazzucato,[11] A. K. McKemey,[5] B. T. Meadows,[7] G. Menegatti,[11] R. Messner,[29] P. M. Mockett,[38] K. C. Moffeit,[29] T. B. Moore,[40] M. Morii,[29] D. Muller,[29] V. Murzin,[20] T. Nagamine,[33] S. Narita,[33] U. Nauenberg,[8] H. Neal,[29] M. Nussbaum,[7] N. Oishi,[21] D. Onoprienko,[32] L. S. Osborne,[19] R. S. Panvini,[37] C. H. Park,[31] T. J. Pavel,[29] I. Peruzzi,[12] M. Piccolo,[12] L. Piemontese,[11] K. T. Pitts,[22] R. J. Plano,[28] R. Prepost,[39] C. Y. Prescott,[29] G. D. Punkar,[29] J. Quigley,[19] B. N. Ratcliff,[29] T. W. Reeves,[37] J. Reidy,[18] P. L. Reinertsen,[35] P. E. Rensing,[29] L. S. Rochester,[29] P. C. Rowson,[9] J. J. Russell,[29] O. H. Saxton,[29] T. Schalk,[35] R. H. Schindler,[29] B. A. Schumm,[35] J. Schwiening,[29] S. Sen,[40] V. V. Serbo,[29] M. H. Shaevitz,[9] J. T. Shank,[6] G. Shapiro,[15] D. J. Sherden,[29] K. D. Shmakov,[32] C. Simopoulos,[29] N. B. Sinev,[22] S. R. Smith,[29] M. B. Smy,[10] J. A. Snyder,[40] H. Staengle,[10] A. Stahl,[29] P. Stamer,[28] H. Steiner,[15] R. Steiner,[1] M. G. Strauss,[17] D. Su,[29] F. Suekane,[33] A. Sugiyama,[21] S. Suzuki,[21] M. Swartz,[14] A. Szumilo,[38] T. Takahashi,[29] F. E. Taylor,[19] J. Thom,[29] E. Torrence,[19] N. K. Toumbas,[29] T. Usher,[29] C. Vannini,[26] J. Va'vra,[29] E. Vella,[29] J. P. Venuti,[37] R. Verdier,[19] P. G. Verdini,[26] D. L. Wagner,[8] S. R. Wagner,[29] A. P. Waite,[29] S. Walston,[22] J. Wang,[29] S. J. Watts,[5] A. W. Weidemann,[32] E. R. Weiss,[38] J. S. Whitaker,[6] S. L. White,[32] F. J. Wickens,[27] B. Williams,[8] D. C. Williams,[19] S. H. Williams,[29] S. Willocq,[17] R. J. Wilson,[10] W. J. Wisniewski,[29] J. L. Wittlin,[17] M. Woods,[29] G. B. Word,[37] T. R. Wright,[39] J. Wyss,[24] R. K. Yamamoto,[19] J. M. Yamartino,[19] X. Yang,[22] J. Yashima,[33] S. J. Yellin,[34] C. C. Young,[29] H. Yuta,[2] G. Zapalac,[39] R. W. Zdarko,[29] and J. Zhou[22]

(SLD Collaboration)

[1]*Adelphi University, Garden City, New York 11530*
[2]*Aomori University, Aomori, 030 Japan*
[3]*INFN Sezione di Bologna, I-40126 Bologna, Italy*
[4]*University of Bristol, Bristol, United Kingdom*
[5]*Brunel University, Uxbridge, Middlesex UB8 3PH United Kingdom*
[6]*Boston University, Boston, Massachusetts 02215*
[7]*University of Cincinnati, Cincinnati, Ohio 45221*
[8]*University of Colorado, Boulder, Colorado 80309*
[9]*Columbia University, New York, New York 10533*
[10]*Colorado State University, Ft. Collins, Colorado 80523*
[11]*INFN Sezione di Ferrara and Universita di Ferrara, I-44100 Ferrara, Italy*
[12]*INFN Laboratory Nazionali di Frascati, I-00044 Frascati, Italy*
[13]*University of Illinois, Urbana, Illinois 61801*
[14]*Johns Hopkins University, Baltimore, Maryland 21218-2686*
[15]*Lawrence Berkeley Laboratory, University of California, Berkeley, California 94720*
[16]*Louisiana Technical University, Ruston, Louisiana 71272*
[17]*University of Massachusetts, Amherst, Massachusetts 01003*
[18]*University of Mississippi, University, Mississippi 38677*
[19]*Massachusetts Institute of Technology, Cambridge, Massachusetts 02139*
[20]*Institute of Nuclear Physics, Moscow State University, 119899 Moscow, Russia*
[21]*Nagoya University, Chikusa-ku, Nagoya 464, Japan*
[22]*University of Oregon, Eugene, Oregon 97403*

[23]*Oxford University, Oxford OX1 3RH, United Kingdom*
[24]*INFN Sezione di Padova and Universita di Padova, I-35100 Padova, Italy*
[25]*INFN Sezione di Perugia and Universita di Perugia, I-06100 Perugia, Italy*
[26]*INFN Sezione di Pisa and Universita di Pisa, I-56010 Pisa, Italy*
[27]*Rutherford Appleton Laboratory, Chilton, Didcot, Oxon OX11 0QX, United Kingdom*
[28]*Rutgers University, Piscataway, New Jersey 08855*
[29]*Stanford Linear Accelerator Center, Stanford University, Stanford, California 94309*
[30]*Sogang University, Seoul, Korea*
[31]*Soongsil University, Seoul 156-743, Korea*
[32]*University of Tennessee, Knoxville, Tennessee 37996*
[33]*Tohoku University, Sendai 980, Japan*
[34]*University of California at Santa Barbara, Santa Barbara, California 93106*
[35]*University of California at Santa Cruz, Santa Cruz, California 95064*
[36]*University of Victoria, Victoria, British Columbia, Canada V8W 3P6*
[37]*Vanderbilt University, Nashville, Tennessee 37235*
[38]*University of Washington, Seattle, Washington 98105*
[39]*University of Wisconsin, Madison, Wisconsin 53706*
[40]*Yale University, New Haven, Connecticut 06511*
(Received 3 March 1999; published 6 October 1999)

The structure of $e^+e^-\to b\bar{b}g$ events was studied using Z^0 decays recorded in the SLC Large Detector experiment at SLAC. Three-jet final states were selected and the charge-coupled device-based vertex detector was used to identify two of the jets as b or $\bar{b}$. Distributions of the gluon energy and polar angle were measured over the full kinematic range for the first time, and compared with perturbative QCD predictions. The energy distribution is potentially sensitive to an anomalous b chromomagnetic moment κ. We measured κ to be consistent with zero and set the first limits on its value: $-0.17<\kappa<0.11$ at 95% C.L.
[S0556-2821(99)01121-2]

PACS number(s): 13.65.+i, 12.38.Qk, 14.65.Fy

The observation of e^+e^- annihilation into final states containing three hadronic jets, and their interpretation in terms of the process $e^+e^-\to q\bar{q}g$ [1], provided the first direct evidence for the existence of the gluon, the gauge boson of the theory of strong interactions, quantum chromodynamics (QCD). In subsequent studies the jets were usually energy ordered, and the lowest-energy jet was assigned as the gluon; this is correct roughly 80% of the time, but preferentially selects low-energy gluons. If the gluon jet could be tagged explicitly, event-by-event, the full kinematic range of gluon energies could be explored, and more detailed tests of QCD could be performed [2]. Because of advances in vertex detection this is possible using $e^+e^-\to b\bar{b}g$ events. The large mass and relatively long lifetime, ~1.5 ps, of the leading B hadron in b-quark jets [3] lead to decay signatures which distinguish them from lighter-quark (u, d, s or c) and gluon jets. We used our 120-million-pixel charge-coupled device (CCD) vertex detector [4] to identify in each event the two jets that contain the B hadrons, and hence to tag the gluon jet. This allowed us to make the first measurement of the gluon energy and polar-angle distributions over the full kinematic range.

Additional motivation to study the $b\bar{b}g$ system has been provided by measurements involving inclusive $Z^0\to b\bar{b}$ decays. Several reported determinations of $R_b=\Gamma(Z^0\to b\bar{b})/\Gamma(Z^0\to q\bar{q})$ and the Z^0-b parity-violating coupling parameter, A_b, have reached a precision below the size of the QCD radiative corrections. A number of these [5] have differed from standard model (SM) expectations at the few standard deviation level. Since one expects new high-mass-scale dynamics to couple to the massive third-generation fermions, these measurements aroused considerable interest and speculation. We have therefore investigated in detail the strong-interaction dynamics of the b quark. We have compared the strong coupling of the gluon to b-quarks with that to light- and charm-quarks [6], as well as tested parity (P) and charge⊕parity (CP) conservation at the $b\bar{b}g$ vertex [7]. Here we study the structure of $b\bar{b}g$ events via the distributions of the gluon energy and polar angle with respect to the beamline. We compare these results with perturbative QCD predictions, including a recent calculation at next-to-leading order (NLO) which takes quark mass effects into account [8].

In QCD the chromomagnetic moment of the b quark is induced at the one-loop level and is of order α_s/π. A more general $b\bar{b}g$ Lagrangian term with a modified coupling [9] may be written

$$\mathcal{L}^{b\bar{b}g}=g_s\bar{b}T_a\left(\gamma_\mu+\frac{i\sigma_{\mu\nu}k^\nu}{2m_b}(\kappa-i\tilde{\kappa}\gamma_5)\right)bG_a^\mu, \qquad (1)$$

where κ and $\tilde{\kappa}$ parametrize the anomalous chromomagnetic and chromoelectric moments, respectively, which might arise from physics beyond the SM. The effects of the chromoelectric moment are sub-leading with respect to those of

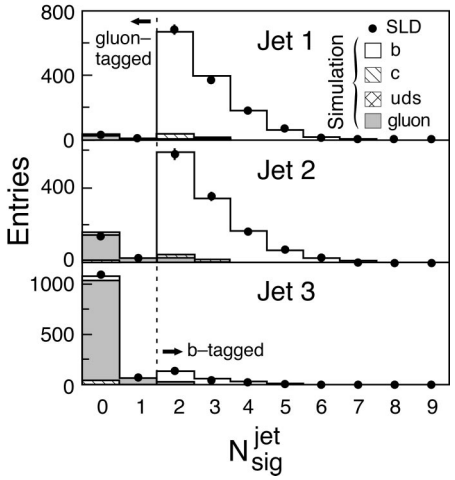

FIG. 1. The $N_{\rm sig}^{\rm jet}$ distributions for jets in $b\bar{b}g$-tagged events, labeled according to jet energy (dots); errors are statistical. Histograms: simulated distributions showing jet flavor contributions.

the chromomagnetic moment, so for convenience we set $\tilde{\kappa}$ to zero. A non-zero κ would modify [9] the gluon energy distribution in $b\bar{b}g$ events relative to the standard QCD case. Hence we have used our data to set the first limits on κ.

We used hadronic decays of Z^0 bosons produced by e^+e^- annihilations at the SLAC Linear Collider (SLC) which were recorded in the SLC Large Detector (SLD) [10]. The criteria for selecting Z^0 decays, and the charged tracks used for flavor-tagging, are described in [6,11]. We applied the JADE algorithm to define jets, using a scaled-invariant-mass criterion $y_{\rm cut}=0.02$ [12]. Events classified as 3-jet states were retained if all three jets were well contained within the barrel tracking system, with polar angle $|\cos\theta_{\rm jet}| \leqslant 0.71$. From our 1993-95 data samples, comprising roughly 150 000 hadronic Z^0 decays, 33 805 events were selected. In order to improve the energy resolution the jet energies were rescaled kinematically according to the angles between the jet axes, assuming energy and momentum conservation and massless kinematics [7]. The jets were then labeled in order of energy such that $E_1 > E_2 > E_3$.

Charged tracks with a large transverse signed impact parameter with respect to the measured interaction point (IP) were used to tag $b\bar{b}g$ events [6]. The resolution on the impact parameter, projected in the plane normal to the beamline, d, is $\sigma_d = 11 \oplus 70/(p_\perp \sqrt{\sin\theta})$ μm, where $p_\perp$ is the track transverse momentum in GeV/c, and θ the polar angle, with respect to the beamline. The flavor tag was based on the number of tracks per jet, $N_{\rm sig}^{\rm jet}$, with $d/\sigma_d \geqslant 3$. Events were retained in which exactly two jets were b-tagged by requiring each to have $N_{\rm sig}^{\rm jet} \geqslant 2$, and in which the remaining jet had $N_{\rm sig}^{\rm jet} < 2$ and was hence tagged as the gluon; 1329 events were selected. The efficiency for selecting true $b\bar{b}g$ events is 8.3%. This was estimated from a simulated event sample generated using the JETSET 7.4 parton shower [13], with parameter values tuned to hadronic e^+e^- annihilation data [14], combined with a simulation of B-decays tuned to $\Upsilon(4S)$ data [15] and a simulation of the detector. The efficiency peaks at about 11% for 15 GeV gluons. Lower-energy gluon jets are sometimes merged with the parent b-jet by the jet-finder. At higher gluon energies the correspondingly lower-energy b-jets are harder to tag, and there is also a higher probability of losing a jet outside the detector acceptance.

TABLE I. Estimated purities of the tagged gluon-jet samples.

Jet label	No. tagged gluon jets	Purity
3	1140	96.1%
2	155	90.2%
1	34	65.7%

For the selected event sample, Fig. 1 shows the $N_{\rm sig}^{\rm jet}$ distributions separately for jets 1, 2 and 3. In about 15% of cases the gluon-tagged jet is not the lowest-energy jet (jet 3). The simulated contributions from true gluons are indicated, and the estimated gluon purities [16] are listed in Table I. The inclusive gluon purity of the tagged-jet sample is 95%. With this sample we formed the distributions of two gluon-jet observables, the scaled energy $x_g = 2E_{\rm gluon}/\sqrt{s}$, and the polar angle with respect to the beamline, θ_g. The distributions are shown in Fig. 2. The simulation is also shown; it reproduces the data.

The backgrounds were estimated using the simulation and are of three types: non-$b\bar{b}$ events, $b\bar{b}$ but non-$b\bar{b}g$ events, and true $b\bar{b}g$ events in which the gluon jet was mistagged as a b-jet. These are shown in Fig. 2. The non-$b\bar{b}$ events ($\sim$5% of the $b\bar{b}g$ sample) are mainly $c\bar{c}g$ events, 90% of which had the gluon correctly tagged. There is a small contribution ($\sim$0.1% of the $b\bar{b}g$ sample) from light-quark events. The dominant background is formed by $b\bar{b}$ but non-$b\bar{b}g$ events. These are true $b\bar{b}$ events which were not classified as 3-jet events at the parton level, but which were misreconstructed and tagged as 3-jet $b\bar{b}g$ events in the detector using the same jet algorithm and $y_{\rm cut}$ value. This arises from the broadening of the particle flow around the original b and $\bar{b}$ directions due

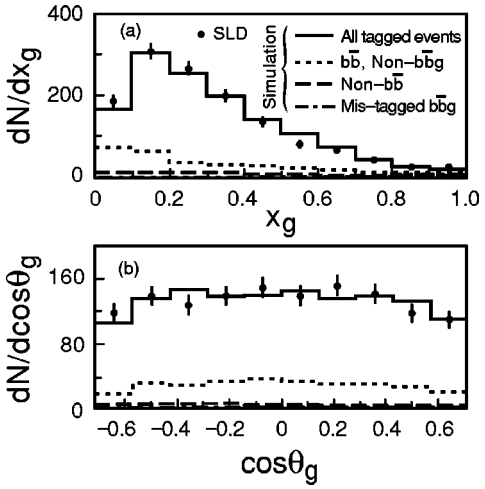

FIG. 2. Raw measured distributions of (a) x_g and (b) $\cos\theta_g$ (dots); errors are statistical. Histograms: simulated distributions including background contributions.

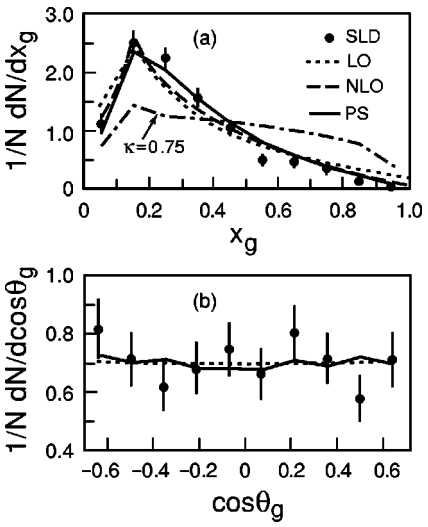

FIG. 3. Corrected distributions of (a) x_g and (b) $\cos\theta_g$ (dots); errors are statistical. Perturbative QCD predictions (see text) are shown as lines joining entries plotted at the respective bin centers.

to hadronization and the high-transverse-momentum B-decay products, causing the jet-finder to reconstruct a ''fake'' third jet, which is almost always assigned as the gluon. The population of such fake gluon jets peaks at low energy [Fig. 2(a)], as expected. Mistagged events comprise less than 1% of the $b\bar{b}g$ sample.

The distributions were corrected to obtain the true parton-level gluon distributions $D^{\rm true}(X)$ by applying a bin-by-bin procedure: $D^{\rm true}(X)=C(X)\ [D^{\rm raw}(X)-B(X)]$, where $X=x_g$ or $\cos\theta_g$, $D^{\rm raw}(X)$ is the raw distribution, $B(X)$ is the background contribution, and $C(X)\equiv D^{\rm true}_{MC}(X)/D^{\rm recon}_{MC}(X)$ is a correction that accounts for the efficiency for accepting true $b\bar{b}g$ events into the tagged sample, as well as for bin-to-bin migrations caused by hadronization, the resolution of the detector, and bias of the jet-tagging technique. Here $D^{\rm true}_{MC}(X)$ is the true distribution for Monte Carlo (MC)-generated $b\bar{b}g$ events, and $D^{\rm recon}_{MC}(X)$ is the resulting distribution after full simulation of the detector and application of the same analysis procedure as applied to the data. The shape-dependent part of the bin-by-bin correction varies slowly and smoothly between roughly 0.8 and 1.2 [11].

As a cross-check, an alternative correction procedure was employed in which bin-to-bin migrations, which can be as large as 20%, were explicitly taken into account: $D^{\rm true}(X_i)=M(X_i,X_j)\ [D^{\rm raw}(X_j)-B(X_j)]/\epsilon(X_i)$, with the unfolding matrix $M(X_i,X_j)$ defined by $D^{\rm true}_{MC}(X_i)=M(X_i,X_j)D^{\rm recon}_{MC}(X_j)$, where true $b\bar{b}g$ events generated in bin i may, after reconstruction, be accepted into the tagged sample in bin j. $\epsilon(X)$ is the efficiency for accepting $b\bar{b}g$ events in bin i into the tagged sample. The resulting distributions of x_g and $\cos\theta_g$ are within the error bands of the respective distributions yielded by the bin-by-bin method.

The fully-corrected distributions are shown in Fig. 3. Since, in an earlier study [6], we verified that the overall rate of $b\bar{b}g$-event production is consistent with QCD expectations, we normalized the gluon distributions to unit area and

TABLE II. χ^2 for the comparison of the QCD predictions with the corrected data.

QCD calculation	χ^2: x_g (10 bins)
LO $m_b(m_Z)=3$ GeV/c^2	73.6
NLO $m_b(m_Z)=3$ GeV/c^2	24.3
PS $M_b=5$ GeV/c^2	9.5

we study further the distribution shapes. The x_g distribution rises, peaks around $x_g\sim 0.15$, and decreases towards zero as $x_g\to 1$. The peak is a kinematic artifact of the jet algorithm, which ensures that gluon jets are reconstructed with a non-zero energy which depends on the y_c value. The $\cos\theta_g$ distribution is flat.

We have considered sources of systematic uncertainty that potentially affect our results. These may be divided into uncertainties in modeling the detector and uncertainties in the underlying physics modeling. To estimate the first case we systematically varied the track and event selection requirements, as well as the tracking efficiency [6,11]. In the second case parameters used in our simulation, relating mainly to the production and decay of charm and bottom hadrons, as well as hadronization, were varied within their measurement errors [11]. For each variation the data were recorrected to derive new x_g and $\cos\theta_g$ distributions, and the deviation with respect to the standard case was assigned as a systematic uncertainty. None of the variations affects our conclusions. All uncertainties were assumed to be uncorrelated and were added in quadrature in each bin of x_g and $\cos\theta_g$. The systematic error in each bin is smaller than the corresponding statistical error.

We compared the data with perturbative QCD predictions for the same jet algorithm and y_c value. We used leading-order (LO) and NLO results based on recent calculations [8] in which quark mass effects were explicitly taken into account; a b-mass value of $m_b(m_Z)=3$ GeV/c^2 was used [17]. We also derived these distributions using the ''parton shower'' (PS) implemented in JETSET. This is equivalent to a calculation in which all leading, and a subset of next-to-leading, $\ln y_c$ terms are resummed to all orders in α_s. In physical terms this allows events to be generated with multiple orders of parton radiation, in contrast to the maximum number of 3 (4) partons allowed in the LO (NLO) calculations, respectively. Configurations with $\geqslant 3$ partons are relevant to the observables considered here since they may be resolved as 3-jet events by the jet-finding algorithm.

These predictions are shown in Fig. 3. The calculations reproduce the measured $\cos\theta_g$ distribution, which is clearly insensitive to the details of higher-order soft parton emission. For x_g, although the LO calculation reproduces the main features of the shape of the distribution, it yields too few events in the region $0.2<x_g<0.5$, and too many events for $x_g<0.1$ and $x_g>0.5$. The NLO calculation is noticeably better, but also shows a deficit for $0.2<x_g<0.4$. The PS calculation describes the data across the full x_g range. The χ^2 for the comparison of each calculation with the data is given in Table II. These results suggest that multiple orders of parton radiation need to be included, in agreement with our earlier

measurements of jet energy distributions using flavor-inclusive Z^0 decays [18]. We also investigated LO and NLO predictions based on matrix elements implemented in JETSET which assume massless quarks. The resulting distributions are practically indistinguishable from the massive ones, even though the large b-mass has been seen [17] to affect the $b\bar{b}g$ event rate at the level of 5%. The effect of varying α_s within the world-average range is similarly small.

We conclude that perturbative QCD in the PS approximation accurately reproduces the gluon distributions in $b\bar{b}g$ events. However, it is interesting to consider the extent to which anomalous chromomagnetic contributions are allowed. The Lagrangian represented by Eq. (1) yields a model that is non-renormalizable. Nevertheless tree-level predictions can be derived [9] and used for a ''straw man'' comparison with QCD. For illustration, the effect of a large anomalous moment, $\kappa = 0.75$, on the shape of the x_g distribution is shown in Fig. 3(a); there is a clear depletion of events in the region $x_g < 0.5$ and a corresponding enhancement for $x_g \geqslant 0.5$. By contrast the shape of the $\cos\theta_g$ distribution is relatively unchanged (not shown), even by such a large κ value. In each bin of the x_g distribution, we parametrized the leading-order effect of an anomalous chromomagnetic moment and added it to the PS calculation to arrive at an effective QCD prediction including the anomalous moment at leading-order. A χ^2 minimization fit was performed to the data with κ as a free parameter, yielding $\kappa = -0.029 \pm 0.070(\text{stat.})^{+0.013}_{-0.003}(\text{syst.})$, which is consistent with zero within the errors, with a χ^2 of 9.3 for 9 degrees of freedom. The distribution corresponding to this fit is indistinguishable from the PS prediction [Fig. 3(a)] and is not shown. Our result corresponds to 95% confidence-level (C.L.) upper limits of $-0.17 < \kappa < 0.11$.

In conclusion, we used the precise SLD tracking system to tag the gluon in 3-jet $e^+e^- \to Z^0 \to b\bar{b}g$ events. We studied the structure of these events in terms of the scaled gluon energy and polar angle, measured for the first time across the full kinematic range. We compared our data with perturbative QCD predictions, and found that the effect of the b-mass on the shapes of the distributions is small, that beyond-LO QCD contributions are needed to describe the energy distribution, and that the parton shower prediction agrees best with the data. We also investigated an anomalous b-quark chromomagnetic moment, κ, which would affect the shape of the energy distribution. We set 95% C.L. limits of $-0.17 < \kappa < 0.11$. As far as we are aware, these are the first such limits on an anomalous quark chromomagnetic coupling.

We thank the personnel of the SLAC accelerator department and the technical staffs of our collaborating institutions for their outstanding efforts on our behalf. We thank A. Brandenburg, P. Uwer, and T. Rizzo for many helpful discussions and for their calculational efforts on our behalf.

[1] See e.g. S. L. Wu, Phys. Rep. **107**, 59 (1984); J. Ellis, M. K. Gaillard, and G. G. Ross, Nucl. Phys. **B111**, 253 (1976); **B130**, 516(E) (1997).
[2] See e.g. P. N. Burrows and P. Osland, Phys. Lett. B **400**, 385 (1997), and references therein. See also OPAL Collaboration, P. D. Acton *et al.*, Z. Phys. C **58**, 387 (1993).
[3] We do not distinguish between particle and antiparticle.
[4] C. J. S. Damerell *et al.*, Nucl. Instrum. Methods Phys. Res. A **288**, 236 (1990).
[5] See e.g., G. C. Ross, in *Electroweak Interactions and Unified Theories*, Proceedings of the XXXI Rencontre de Moriond, Les Arcs, Savoie, France, 1996, edited by J. Tran Thanh Van, (Editions Frontieres, Gif-sur-Yvette, 1996), p. 481; D. Abbaneo *et al.*, CERN-PPE-97/154, 1997.
[6] SLD Collaboration, K. Abe *et al.*, Phys. Rev. D **59**, 012002 (1999).
[7] SLD Collaboration, K. Abe *et al.*, SLAC-PUB-7823, 1998.
[8] W. Bernreuther, A. Brandenburg, and P. Uwer, Phys. Rev. Lett. **79**, 189 (1997); A. Brandenburg and P. Uwer, Nucl. Phys. **B515**, 279 (1998).
[9] T. Rizzo, Phys. Rev. D **50**, 4478 (1994); and (private communications).
[10] SLD Design Report, SLAC Report 273, 1984.
[11] P. J. Dervan, Ph.D. thesis, Brunel University; SLAC-Report-523, 1998.
[12] JADE Collaboration, W. Bartel *et al.*, Z. Phys. C **33**, 23 (1986). This algorithm has been used extensively in e^+e^- annihilation studies for many years. In detailed simulation studies including other jet algorithms we found that it, with $y_c = 0.02$, yields the optimal performance of our impact-parameter-based flavor-tagging procedure.
[13] T. Sjöstrand, Comput. Phys. Commun. **82**, 74 (1994).
[14] P. N. Burrows, Z. Phys. C **41**, 375 (1988); OPAL Collaboration, M. Z. Akrawy *et al.*, *ibid.* **47**, 505 (1990).
[15] See references in SLD Collaboration, K. Abe *et al.*, Phys. Rev. Lett. **79**, 590 (1997).
[16] We expect less than 0.4% of the selected sample to comprise events of the type $e^+e^- \to q\bar{q}g$, with $g \to b\bar{b}$. We expect no events to have been selected in which a tagged jet contains both true b-quarks. In the evaluation of the purity only true $b\bar{b}$ $b\bar{b}$ events were considered as signal $b\bar{b}g$ events; $q\bar{q}$ $b\bar{b}$ events ($q \neq b$) were considered as backgrounds.
[17] See, e.g., P. N. Burrows, in Proceedings of the XXIX International Conference on High Energy Physics, Vancouver, Canada, 1998, p. 728.
[18] SLD Collaboration, K. Abe *et al.*, Phys. Rev. D **55**, 2533 (1997).